Design Method of Coils for Dynamic Wireless Power Transfer Considering Average Transmission Power and Installation Rate

Yuto YAMADA
Faculty of Science and Technology
Tokyo University of Science
Noda, Japan
yuto.yamada20@gmail.com

Kanta SASAKI
Faculty of Science and Technology
Tokyo University of Science
Noda, Japan

Takehiro IMURA
Faculty of Science and Technology
Tokyo University of Science
Noda, Japan

Yoichi HORI
Faculty of Science and Technology
Tokyo University of Science
Noda, Japan

***Abstract*—Several papers have examined the power requirements for Dynamic Wireless Power Transfer (DWPT), but none have compared all types of vehicles and designed appropriate coils. In this paper, a new quasi-optimal load was adopted to make the SS circuit more usable, and in optimizing the transmission coil, the economically best one was adopted considering the average efficiency and the coil installation rate. Although a trade-off between the average transmission efficiency and the coil installation rate was shown, the reduction in the number of coils installed with the coil installation rate was shown to be very dominant compared to the efficiency. As a result, it was found that with more economical coils, a 25-ton truck could be driven 800 km, and a light-duty vehicle could be driven without considering its range.**

Keywords—Dynamic Wireless Power Transfer, Coil design Inductive Charging, Class 8 truck, Coil Installation rate.

I. INTRODUCTION

Wireless Power Transfer (WPT), which transfers power to any device without cables, has been the focus of increasing research [1]. Though electric vehicles are expected to attract more attention for their environmental performance and energy conversion efficiency, they face many challenges [2] [3] such as range, price, and vehicle weight. Wireless power transfer to electric vehicles can be used to power any vehicle, and in particular, dynamic wireless power transfer can contribute to extending the cruising range [4-6], since power is transferred from the road while the vehicle is in motion, without the need for a large battery. Power supply while driving can be either on the highway or in the city [7], but in this paper, we focus on wireless power transfer while driving on the highway. Many papers focus on the power supply to large trucks and buses [8-10], which have large transportation volumes, and there are few references that consider power transfer to all kinds of vehicles. In addition, although there are many technical studies [11-13] and economics oriented papers [14-17] on wireless power transfer to electric vehicles, there is still no literature that actually sets the power to be sent to the vehicle, designs the coil, and considers the coil installation rate. It is considered that charging facilities will be installed in the electric road, etc., but it may be difficult to arrange them evenly. It is important to consider the efficiency and power of the entire electric roadway, since the transmission efficiency and power vary while passing over the coils. In this paper, we design a wireless electric road considering the average efficiency and the average power transmission of 22 kVA class, and describe the cruising range of various vehicles from large vehicles to small vehicles on Japanese highways. The economic impact of the length of the power transmission coils is discussed, and it is shown that it is important to reduce the coil installation rate and the number of coils installed in the electric road.

Chapter 2 explains how to calculate the power requirements of the vehicles, Chapter 3 explains the constraints on the number of power receiving coils that can be installed in each vehicle, Chapter 4 explains the theoretical equation of the SS circuit and the quasi-optimal load adopted in this study, and then optimizes the power transmission coils. In Chapter 5, the distance that each vehicle can travel when the proposed coils are placed is explained, and in Chapter 6, the economic impact of the power transmission efficiency and the number of coils installed on a 30-year operation is discussed. Finally, Chapter 7 presents the conclusions.

II. DERIVATION OF VEHICLE TRACTION FORCE

One of the objectives of this paper is to propose electric roads that can travel a 25-ton truck, the largest commercial vehicle in Japan, for 800 km from the viewpoint of convenience with Internal Combustion Engine Vehicles (ICEV). Therefore, it is essential to derive the power consumption of the vehicle during driving in order to design the coil. In this chapter, we introduce the main vehicles running in Japan and show how to derive the power consumed by these vehicles at high speed (80km/h). Nissan LEAF, an EV already on the market, was used for the light-duty vehicle [18]. The light-duty truck is ISUZU ELF [19], the medium-duty truck is ISUZU FORWARD [20], the highway bus is Hino Motors SELEGA [21], and the heavy-duty truck (25-ton: Class 8) is ISUZU GIGA [22]. However, each of the vehicles introduced here is currently an internal combustion engine vehicle, and the equations used to derive them are simple because the calculations are based on the assumption that the vehicles will become EVs. In Japan, there are a large number of mini cars, but these cars consume even less power than passenger cars (light-duty vehicles), so they were ignored in this study. The amount of energy lost by the battery, $E_{discharge}$, is obtained by considering the mechanical power conversion efficiency η_{mec}, motor drive efficiency η_{motor}, and inverter conversion efficiency η_{inv}.

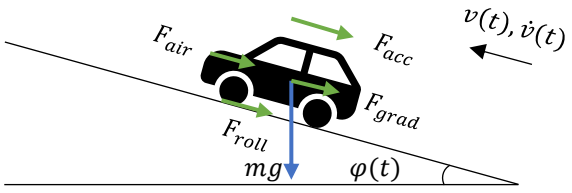

Fig. 1 Resistance force applied to the driving vehicle.

Considering the driving environment as shown in Fig. 1, the tractive force $F(t)$ that pulls the vehicle forward can be expressed as (1) using the acceleration resistance F_{acc}, rolling resistance F_{roll}, gradient resistance F_{grad}, and air resistance F_{air} [14] [17] [23].

$$\begin{aligned} F(t) &= F_{acc}(t) + F_{roll}(t) + F_{grad}(t) + F_{air}(t) \\ &= m\dot{v}(t) + \mu_{rr} mg\cos\varphi(t) + mg\sin\varphi(t) \\ &\quad + \frac{1}{2}\rho C_d A(v(t) - v_{wind}(t))^2 \end{aligned} \tag{1}$$

The rotating part equivalent mass that acts on the acceleration resistance is ignored in this study because it does not consider acceleration and requires separate and complicated calculations for each vehicle. In addition, although there is a resistance $F_{curvature}$ generated at the time of a curve in actual driving, it is ignored in this study. μ_{rr} is the rolling resistance coefficient of the tire, ρ [kg/m^3] is the air density, C_d is the aerodynamic drag coefficient, A [m^2] is the total projected area, φ is the gradient.

The force $F(t)$ required for the vehicle to move forward has been obtained by (1). In this chapter, we will calculate the amount of electricity that the electric vehicle actually consumes during driving and derive the remaining battery power when the power is supplied by wireless power transfer. When an electric vehicle is traveling at speed $v(t)$ and acceleration $\dot{v}(t)$, the power $P(t)$ to pull the vehicle and the amount of electricity E required in T seconds can be expressed by (2) and (3).

$$P(t) = F(t)v(t) \tag{2}$$

$$E = \int_0^T P(t)dt \tag{3}$$

This allows the energy consumed by the battery, $E_{discharge}$, to be expressed as (4). The flow from the power source to the energy consumed by the vehicle tail is shown in Fig. 2, and the energy conversion efficiency at each component is shown. Table 1 also summarizes each conversion efficiency [24]. η_{wpt} is not shown because it differs depending on the coil.

Table 1 Loss generated by each element.

	η_{inv}	η_{wpt}	η_{rec}	$\eta_{battery}$	η_{motor}	η_{mec}
Efficiency	0.98	0.95	0.95	0.98	0.90	0.97

$$E_{discharge} = \frac{E}{\eta_{mec}\eta_{motor}\eta_{inv}\eta_{battery}} \tag{4}$$

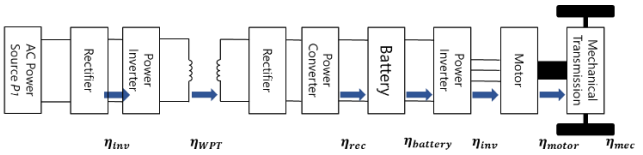

Fig. 2 The main losses of electric vehicles with wireless power transfer.

Next, the power transferred from the AC power source to the EV by wireless power transfer is $P_1(t)$, the amount of energy charged to the battery, E_{charge}, is represented by (5).

$$E_{charge} = \int_0^T P_1(t)\eta_{inv}\eta_{wpt}\eta_{rec}dt \tag{5}$$

Therefore, the increase or decrease of the remaining battery capacity ΔC_δ can be expressed as (6).

$$\Delta C_\delta = E_{charge} - E_{discharge} \tag{6}$$

Table 2 shows the specifications of the vehicle types used to calculate the power requirements of each vehicle at high speed. In the case of the truck, a C_d value of 0.6 was used [14], as many C_d values are not published. About TESLA SEMI [25], which is about to be released, the C_d value is 0.36, so we used a strict condition for this calculation.

From the above, the power requirements for high-speed driving are summarized in Table 3.

Table 3 Power consumption per each vehicle. (Each vehicle drives at a speed of 80 km/h.)

Light duty vehicle	Class 3 truck	Class 5 truck	Coach	Class 8 truck
10kW	39kW	47kW	80kW	100kW

This means that Class 8 trucks consume much more energy than light-duty vehicles. Dynamic wireless power transfer is a technology that extends the cruising range while reducing the onboard battery by charging while driving. In order to drive a large vehicle that consumes a lot of energy for a long distance, it is necessary to transfer a large amount of power to extend the cruising range. However, designing a coil with a power transmission capacity of 100 kW or more is difficult from the viewpoint of EMC and power supply equipment such as inverters, and in many cases, high power transmission is not economical because it is over-specified for driving light-duty vehicles. Therefore, multiple coils are installed in large vehicles to cover the required power. This will reduce the design and installation costs.

Table 2 Specifications of the verified vehicle.

	Light-duty vehicle	Class 3 truck	Class 5 truck	Coach	Class 8 truck
Type	Nissan leaf S	ISUZU ELF	ISUZU FORWARD	HINO SELEGA	ISUZU GIGA
Gross Vehicle Weight (GVW): m [kg]	1,765	4,775	7,900	15,715	24,820
Length: *L* [mm]	4,480	4,990	8,485	11,990	11,950
Hight: *H* [mm]	1,540	3,055	2,550	3,750	2,490
Width: *B* [mm]	1,790	1,890	2,260	2,490	3,035
Air drag coefficient: C_d	0.28	0.6	0.6	0.55	0.6
Front surface area: *A* [m^2]	2.5	5.7	5.7	9.3	7.5
Battery capacity : C_δ [kWh]	40	75	120	250	400
Rolling resistance coefficient: η_{rr}	0.01	0.01	0.01	0.01	0.01
Air density: ρ [kg/m^3]	1.2	1.2	1.2	1.2	1.

III. Number of Power Receiving Coils That Can Be Equipped on a Vehicle

As mentioned in the previous chapter, large vehicles are equipped with a large number of power receiving coils to cover their power consumption. However, there is a constraint to the number of coils that can be installed due to the length of the vehicle and EMC considerations. In this paper, the size of the coils on the transmission side is one of the parameters to be changed, since this is the design of a wireless electric road. The equation (7) defines the constraints of the power transmission coil size L (in the direction of travel) based on the vehicle length $L_{vehicle}$ and the number of installed power receiving coils n. Since power is transferred when the vehicle body passes over the coil, if the receiving coil is located at the edge of the vehicle body, there is a possibility that a large magnetic field will flow into the vehicle body. Therefore, a space larger than the length of the power transmission coil should be left at the front and rear of the vehicle body. Also, in order to eliminate unintended coupling from the power transmission coil, the power receiving coil should be installed at a distance of at least 1.5 times the length of the power transmission coil L. (9) is expected to be changed as cross-coupling cancellation technology develops in the future. (8) shows that the coil length should be less than 2 m from the viewpoint of magnetic field leakage because the length of a light-duty vehicle body is around 4 m. Fig. 3 shows each parameter.

$$L_{vehicle} \geq 2L + \frac{3}{2}(n-1)L \tag{7}$$

$$L \leq 2000\ [mm] \tag{8}$$

$$D_{Tx}, D_{Rx} \geq \frac{3}{2}L \tag{9}$$

IV. Design of Optimal Power Taransmission Coil

In this chapter, we consider dynamic wireless power transfer in the SS circuit, in which a resonant capacitor is connected in series with the coil used for power transfer, as shown in Fig. 4. The input voltage was 600 V and the frequency was 85 kHz.

A. Theoretical equations and quasi-optimal loads in SS circuits

In the SS circuit, the resonance condition is shown in (10).

$$\omega_0 = 2\pi f = \frac{1}{\sqrt{L_1 C_1}} = \frac{1}{\sqrt{L_2 C_2}} \tag{10}$$

Under resonant conditions, I_1 and I_2 can be expressed as (11) and (12).

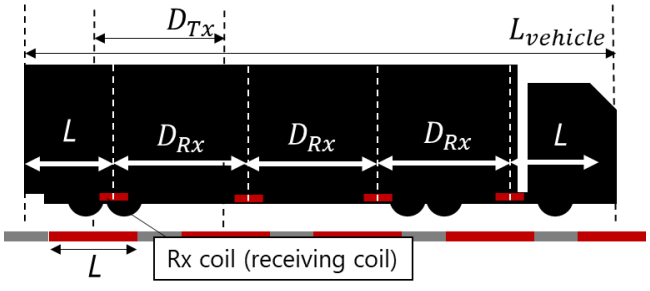

Fig. 3 Definition of various lengths.

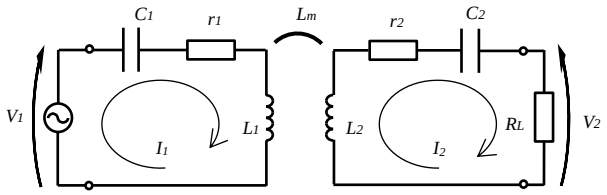

Fig. 4 Equivalent circuit in magnetic field resonance coupling of (S-S).

$$I_1 = \frac{r_2 + R_L}{r_1(r_2 + R_L) + (\omega_0 L_m)^2} V_1 \tag{11}$$

$$I_2 = -\frac{\omega_0 L_m}{r_1(r_2 + R_L) + (\omega_0 L_m)^2} V_1 \tag{12}$$

Power transmission efficiency η and receiving power P_2 can be expressed by (13) and (14).

$$\eta = \frac{R_L(\omega_0 L_m)^2}{(r_2 + R_L)\{r_1(r_2 + R_L) + (\omega_0 L_m)^2\}} \tag{13}$$

$$P_2 = \frac{R_L(\omega_0 L_m)^2}{\{r_1(r_2 + R_L) + (\omega_0 L_m)^2\}^2} V_1^2 \tag{14}$$

The SS circuit has a weakness in that a large current flows when a misalignment occurs. If either I_1 or I_2 exceeds the allowable current, the power transmission has to be stopped. Therefore, a quasi-optimal load R_L' is proposed to reach the allowable current at the same time when misalignment occurs by considering the ratio of the allowable current of I_1 or I_2.

If the allowable currents of primary and secondary are $I_{1,max}$ and $I_{2,max}$, respectively, the quasi-optimal load R_L' can be expressed as (15) using (11) and (12). β is the ratio of allowable currents (16).

$$R_L' = \frac{\omega_0 L_m}{\beta} - r_2 \tag{15}$$

$$\beta = \frac{I_{2,max}}{I_{1,max}} \tag{16}$$

In general, the optimal load is often connected in wireless power transfer, but in dynamic wireless power transfer, the quasi-optimal load R_L' is a very convenient load because high power is required rather than efficiency and misalignment occurs. A detailed explanation will be given later.

The internal resistance of the coil r_i (i = 1, 2) is derived by numerical analysis using the PEEC method, and the mutual inductance L_m is derived by numerical analysis using the Neumann equation [26-27].

B. Determining the optimal transmission coil

In this section, the assumed environment of wireless power transfer is described, and then the appropriate power transmission coil is determined. The distance between coils was 200 mm, and the size of the receiving coil was 420 x 420 mm, which is WPT1/Z3 as specified in SAE J2954 [28]. Litz wire with a strand diameter of 0.05 mm, 10,000 strands, and a finished diameter of 7.85 mm was used with an allowable current of 96 A.

Since the coils on the power receiving side have little effect on the power in the SS circuit [27], we set the pitch to 10.85 mm and set the coil with the highest Q value. A pitch of 7.85 mm would have given a higher Q value, but from the viewpoint of insulation and heat dissipation, a pitch of 10.85 mm was chosen. The length of the transmission side coil in

the vehicle width direction was set to 600 mm, since the power transfer to small vehicles was also considered at the same time. The parameters to be designed are the size of the transmission coil L (600-2000 mm in the direction of travel), the number of turns, and the pitch (10.85-22.85 mm). The optimum coil in this study is the one that can reduce the coil installation rate γ the most. Fig. 5 shows the efficiency, current I_1, I_2 and output power P_2 when the coil size L is 2000mm, pitch is 10.85mm and number of turns is 12.

Since a quasi-optimal load R_L' is set, it can be seen that $I_1$and I_2 both reach the allowable current at the same time, and the transmission section (SWon section) can be extended sufficiently. Fig. 5 shows only one half of the coil, but since the same graph can be obtained for the other half, we will discuss only one side for simplicity. Assuming that the section where power can be transmitted depends only on the allowable current on the primary and secondary sides, I_1 and I_2, the SWon section can be determined from the graph. The horizontal axis of the graph is the position x. If the vehicle is traveling at a constant speed $v(t)$, the amount of power received in the SWon section, E_{SWon}, can be expressed as (17). (17) shows that the areas of the orange and green regions of Fig. 5 are equal.

$$E_{SWon} = \int_0^{SWon} P_2(x)\frac{1}{v}dx \tag{17}$$

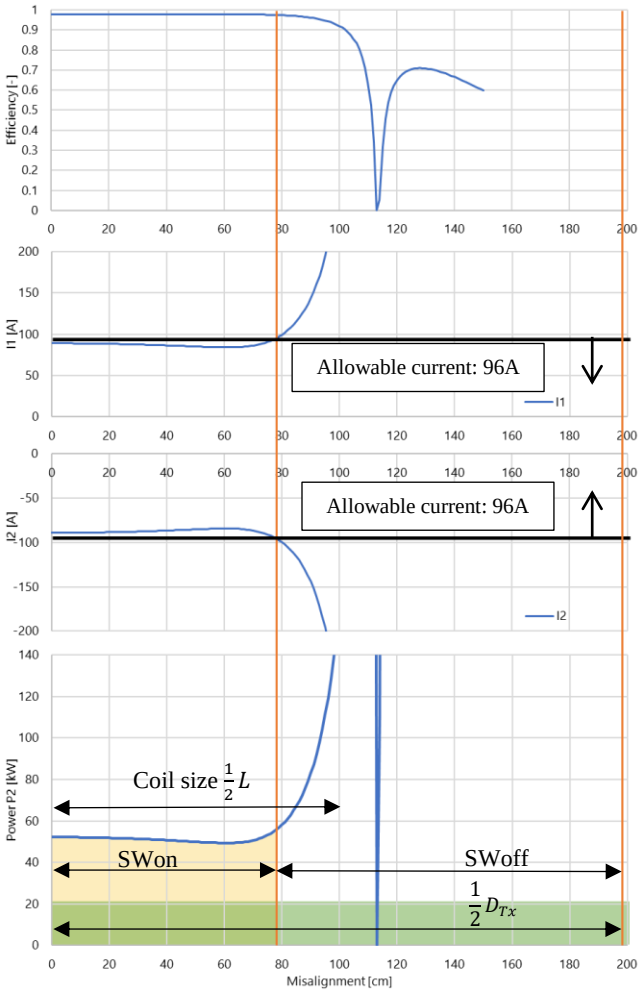

Fig. 5 Efficiency η, current $\boldsymbol{I_1}$, $\boldsymbol{I_2}$ and output power $\boldsymbol{P_2}$ when misalignment occurs. (Orange area: Actual power received. Green area: Area to be covered when the unit is set to receive 20.5 kW of power on average.)

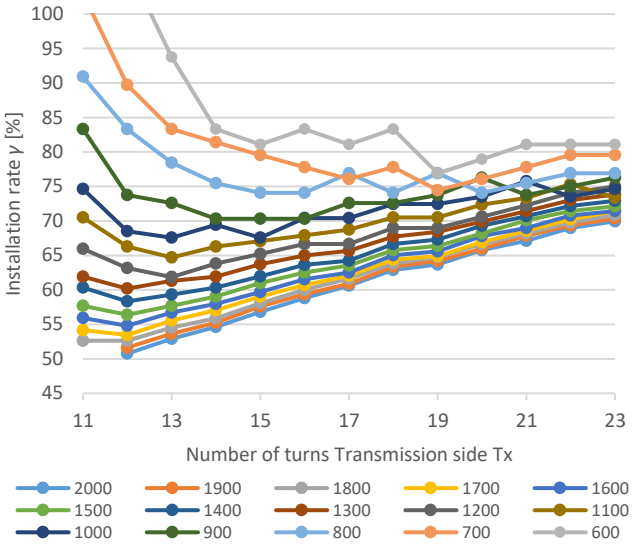

Fig. 6 Installation rate with different number of turns for each coil size. (Pitch:10.85mm, P_{ave}=20.5kW)

On the other hand, if the average power that the vehicle wants to receive is P_{ave}, the distance D_{Tx} that one coil is to cover can be expressed as the distance where (18) holds. Coil installation rate γ represents how much of the coil is buried in the electric road and can be expressed by (19) using the transmission coil length L.

$$E_{SWon} = \int_0^{\frac{1}{2}D_{Tx}} P_{ave}\frac{1}{v}dx \tag{18}$$

$$\gamma = \frac{L}{D_{Tx}} \tag{19}$$

In Fig. 6 below, the pitch is set to 10.85 mm and the coil installation rate γ is evaluated for the coil size L and number of turns. The average power P_{ave} is assumed to be 20.5 kW. In the analysis, the pitch was changed from 10.85 mm to 22.85 mm in 1 mm increments, and the same evaluation was performed for each pitch. As a result of the analysis, it is found that the coil installation rate γ is best reduced to 50.7% when the coil size is 2000 mm, the pitch is 10.85 mm, and the number of turns is 12, as shown in Fig. 6.

Fig. 7 shows the relationship between misalignment and efficiency at the coil with the lowest coil installation rate γ for each coil size L. It is obvious that the larger the coil size, the larger the area of high efficiency. Fig. 7 shows that the peak efficiency value is slightly higher for smaller coil sizes. Fig. 8 shows the average efficiency and the number of coils

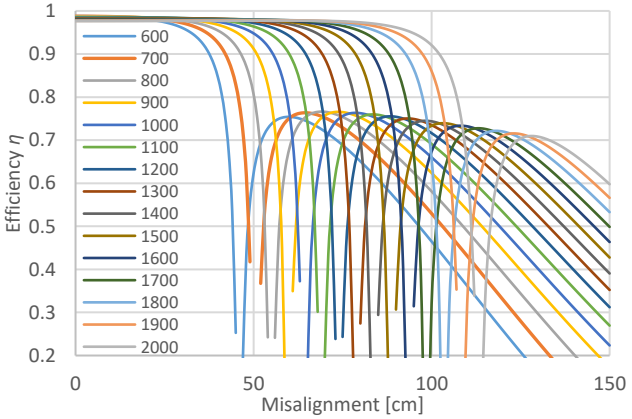

Fig. 7 Relationship between misalignment and efficiency for each coil size L.

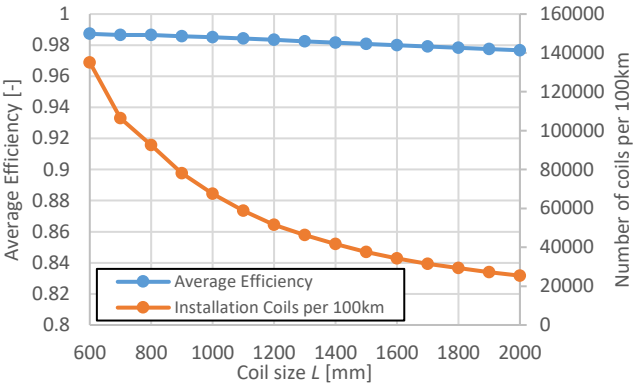

Fig. 8 Relationship between average efficiency and the number of coils installed per 100 km.

installed per 100 km for the coils with the lowest coil installation rate γ for each coil size. The average efficiency decreases slightly as the coil size increases, but the coil installation rate γ can be reduced and the number of coils installed per 100 km can be greatly reduced. Even if the system is operated for 30 years, the effect of reducing the installation cost of the coils is greater than the electricity loss over 30 years. Therefore, it is very important to reduce the number of coils installed by considering the coil size L and coil installation rate γ. The detailed explanation is given in Chapter 6.

V. Driving Range with Dynamic Wireless Power Transfer by Vehicle Type

In Chapter 4, the optimum coil and coil installation rate γ when the average power P_{ave} is 20.5 kW were obtained. In this section, we will simply derive the distance that can be traveled by major vehicles running in Japan when applying electric roads with an average power P_{ave} of 20.5 kW. The driving conditions are 80 km/h at a constant speed in a straight line with no gradient. A one-hour break was taken every four hours, during which time power was supplied while the vehicle was stopped. The number of power receiving coils that can be installed was determined according to (7).

A. Light-duty vehicles

Fig. 9 shows the relationship between the cruising range of a light-duty vehicle and its battery capacity. Since the power supplied to the light-duty vehicles is greater than the power consumed during driving, it can be seen that the car receives more power than its capacity, although it is not actually recharged. One of the weaknesses of EVs is that they consume a large amount of electricity for heating and cooling.

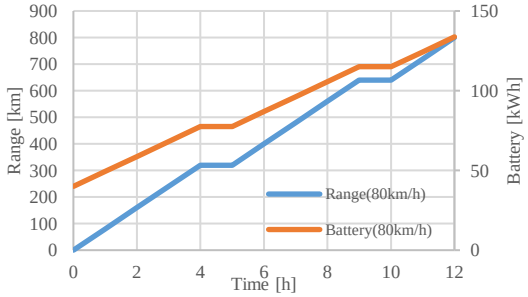

Fig. 9 Relationship between driving distance and the level of battery power of a light duty vehicle. (One power receiving coil installed, no power supply while stationary).

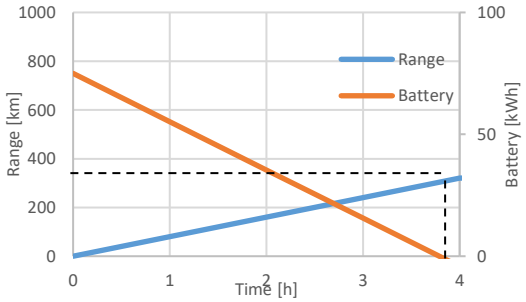

Fig. 10 Relationship between driving distance and the level of battery power of a Class 3 truck. (One power receiving coil installed.)

Recently, the introduction of low-power-consumption heat pump air conditioners has been studied as a substitute for conventional PTC heaters, but they still consume about 2 kW of electricity [29]. When driving without wireless power transfer, the cruising range is reduced by about 20 km when the air conditioning is activated, but at the same time it can be said that wireless power transfer eliminates the need to consider the cruising range.

B. Class 3 truck

Fig. 10 shows the relationship between the cruising range of a light-duty truck and its battery capacity. Compared to light-duty vehicles, light-duty trucks do not have as long a vehicle body, cannot be equipped with multiple power receiving coils, and consume almost four times as much power as light-duty vehicles, resulting in a cruising range of only about 300 km. For light-duty trucks in the 4-ton class, the percentage of operators with a driving range of less than 300 km per operation is about 60% [30]. The ELFs being tested in this study are in the 2-ton class, so the opportunities for long-distance operation are expected to decrease further, and if a longer range is desired, the onboard battery capacity may be increased. On the other hand, if we wanted to achieve a range of 300 km without dynamic wireless power transfer, we would need a 150kWh battery. In other words, if we assume the weight of the battery to be 150Wh/kg, we can reduce the weight of the battery by about 500kg from 75kWh this time [16], which is equivalent to 25% of the weight of a 2-ton load, and we can also say that we have improved the power cost.

C. Class 5 truck

Fig. 11 shows the relationship between the cruising range of a medium-duty truck and its battery capacity. Because of the length of the medium-duty truck, two coils were installed to receive 41kW of power while the truck was driving. One coil was used to supply power while the truck was stationary.

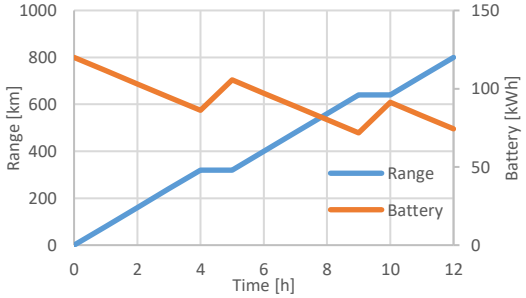

Fig. 11 Relationship between driving distance and the level of battery power of Class 5 truck. (Two power receiving coil installed, power supply while stationary).

This shows that even after 12 hours of operation and 800 km of driving, the truck still has enough battery capacity to drive in the city after exiting the highway. Since medium-duty trucks play a role not only in inter-city transportation but also intra-city transportation, we believe that this result is very beneficial. On the other hand, it is also possible to reduce the battery capacity to increase the load capacity and improve the power cost.

D. Coach

Fig. 12 shows the relationship between the cruising range of a coach (highway bus) and its battery capacity. Because of the long body of the coach, three power receiving coils are installed, and the bus receives 61.5 kW of power during driving. When the bus is stopped, 61.5 kW is charged in the same way. In addition, we set the stopping time of each coach to 30 minutes. This made it possible to travel 800 km in 11 hours, assuming the coach runs at 80 km/h.

E. Class 8 truck

Fig. 13 shows the relationship between the cruising range of a heavy-duty truck and its battery capacity. Since the body of a heavy-duty truck is long, it is equipped with three power receiving coils and receives 61.5kW of power through wireless power supply. This enables the truck to travel 800km in 12 hours. Although the battery can be fully recharged in a little more than 6 hours at each destination or office, commercial vehicles have a very high operating rate [30]. Further charging output is required for power supply while commercial vehicles are stopped.

TESLA is expected to release a GVW 36-ton class SEMI as a Class 8 truck, which is said to have an aerodynamic drag coefficient C_d value of 0.36 and a range of 800 km with a battery capacity of less than about 1 MWh [25]. The 25-ton truck is lighter than the 36-ton SEMI, but the battery size has been reduced by more than half. In addition, a significant reduction in the aerodynamic drag coefficient C_d from the current 0.6 to about 0.36 would lead to a further increase in range and a reduction in battery size.

VI. Efficiency or Number of Coils ?

As a way to reduce the coil installation rate γ, it is possible to reduce the average power P_{ave} from (18) and (19).The objective of this study is to design a electric road for a 25-ton truck with a body length $L_{vehicle}$ of 12 m, traveling 800 km. It can be seen from (7) that the maximum number of coils that can be installed in this vehicle is three if the coils are 2000 mm.

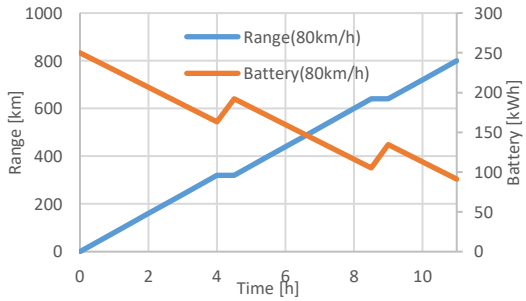

Fig. 12 Relationship between driving distance and the level of battery power of Coach. (Three power receiving coil installed, power supply while stationary).

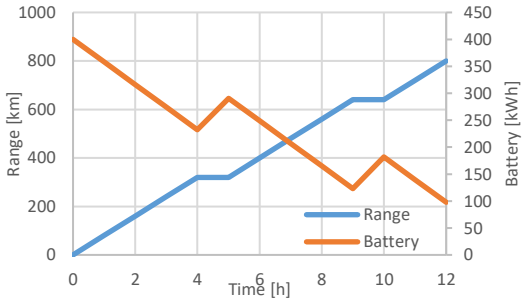

Fig. 13 Relationship between driving distance and the level of battery power of Class 8 truck. (Three power receiving coil installed, power supply while stationary).

However, by changing the coil size L to 1800 mm, four power receiving coils can be installed, and the average power P_{ave} can be reduced to 15.4 kW with four power receiving coils compared to 20.5 kW with three power receiving coils. Therefore, the number of installed coils for the electric road can be significantly reduced. Table 4 compares the case where the coil length L is 1800 mm and the average power P_{ave} is 15.4 kW, the case where the coil length L is 1800 mm and the average power P_{ave} is 20.5 kW, and the case where the coil length L is 2000 mm and the average power P_{ave} is 20.5 kW. When the average power received by one coil, P_{ave}, is equal, comparing the coils in (ii) and (iii), the number of coils installed per km can be reduced, although the efficiency of the longer coil length L is slightly lower.

Table 4 Average efficiency and laying ratio for each coil type.

	Coil Size L [mm]	Average efficiency η_{ave} [%]	Average Power P_{ave} [kW]	Installation rate γ [%]	Number of coils per 1km
(i)	1800	97.83	15.4	39.4	220
(ii)	1800	97.83	20.5	52.6	293
(iii)	2000	97.67	20.5	50.7	254

Here, a brief discussion of the economic benefits of changing the coil size in terms of efficiency and the number of coils installed is presented. The price of a coil is roughly divided into the cost of the Litz wire used, the resonant capacitor, and the resin used in the coil case. The price of Litz wire is about 10 to 15 times the trading price of copper, and the price was set at 10 times in anticipation of a future decline in the price of Litz wire. The price of Litz wire can be determined by the length of the Litz wire line used for the selected coil. The price of the resonant capacitor was set at ¥200,000, because wireless power transfer requires a high withstand voltage for the capacitor and a durability of 20 to 30 years. The resin used for the coil case is polycarbonate, and the price is calculated per volume. Electricity charges are mainly divided into a basic charge and an additional charge based on the amount of electricity used. In order to compare the electricity cost loss due to the loss of efficiency caused by the change in coil size L, the calculation is based on the amount of electricity used only. Assuming wireless power transfer operated for 30 years on 100 km of Japan's Tohoku Expressway, it was calculated whether the number of coils or their efficiency would be more economical.

Compared to the coil in (ii), the cost of electricity for the coil in (iii) would be about ¥40,000,000 higher over 30 years. On the other hand, the difference in the installation cost of the coils was found to be about ¥1,100,000,000, which is a significant reduction. The difference of almost two orders of

magnitude shows that it is more important to reduce the number of coils installed and the cost of coils than the power transmission efficiency even for 30 years of operation. In addition, the number of coils installed can be greatly reduced by lowering the average transmission power P_{ave}, as shown in the coil in (i), but careful consideration is necessary because reducing the average power increases the dependency on the feeder path and causes traffic jams. Table 5 summarizes the amounts used in the calculations.

Table 5 Examples of amounts used for comparison

Copper [¥/kg]	Litz wire [¥/kg]	Coil case (PC) [¥/cm^3]	Electricity charges [¥/kWh]
1,000	10,000	1.75	17

VII. Conclusion

In this study, the energy consumed by various vehicles running in Japan at high speed was derived, and a wireless electric road was proposed that would allow a 25-ton Class 8 truck, which consumes the most power, to achieve a cruising range of 800 km. In the SS circuit, in the case of the coil in (iii) which has the coil length L is 2000 mm and the number of turns is 12 and the pitch is 10.85mm, the average power transmission efficiency is 98.0% and the coil installation rate γ is 96.1% when the optimal load is proposed, while the average efficiency is 97.6% and the coil installation rate γ is 50.7% when the quasi-optimal load R_L' is adopted. The number of coils that can be reduced is nearly 230 per kilometer, which dramatically reduces the cost of coil installation, although the efficiency worsens. In addition, the equation is much simpler than that of the optimal load, so it will be easier to control.

An equation was defined for the constraint on the number of coils installed for receiving power relative to the length of the vehicle and the length of the coils, and it was shown that a 25-ton Class 8 truck could travel 800 km with a low coil installation rate γ. The calculation method of the cruising distance is very simple, but the aerodynamic drag coefficient and other factors are strictly adopted, and it might be possible to travel more than 800 km. By determining the arrangement of the receiving coils as in the proposed (7), it is possible for all types of vehicles in the future to wireless power transfer to multiple coils simultaneously from the same transmission coil while the vehicle is stationary. In addition to Class 8 trucks, many other vehicles were able to achieve a range of 800 km. However, the range of light-duty trucks did not reach 800 km due to their short body length L and the small number of coils that can be installed. In this verification, the same power receiving coil was used for all the vehicles, and the transmission distance was the same, but in reality, the size of the installed power receiving coil and the vehicle height differ for each vehicle, so if the vehicle side can be made more high-power, it is not impossible to extend the cruising distance.

In Chapter 6, the cost of coils and electricity rates were compared in a simplified way to determine whether efficiency or coil installation rate γ should be economically more important, and it was found that the reduction in efficiency did not have a significant impact even considering 30 years of operation and that the reduction in the number of coils installed and the cost of individual coils was very important.

Finally, two types of optimal coils and their arrangement were proposed in this study. The first one (iii) is an electric road with an average power of 20.5 kW using 2000 mm coils in the coil pattern. The average input power is reduced to WPT4 (22kVA). The second pattern is (i), where the average power is reduced to 15.4 kW using 1800 mm coils, and the number of coils installed is reduced the most. In this pattern, a large truck can travel 800 km, but because the average power received is small, the time spent on the road by light-duty vehicles and other vehicles will be longer, resulting in more traffic jams or the need to increase the number of wireless electric road lane from the viewpoint of convenience. It is most important to set the appropriate average power in consideration of the equipment cost other than the coil installation cost, EMC, the ratio of vehicles running on the road, and convenience, etc., when designing the wireless electric road.

Future work will include changes in the characteristics when the vehicle is actually buried in the ground [31], and examining the different vehicle heights of each vehicle.

REFERENCES

[1] A. Kurs, A. Karalis, R. Moffatt, J. D. Joannopoulos, P. Fisher, and M. Soljacic, “Wireless Power Transfer via Strongly Coupled Magnetic Resonances,” Science, Vol. 317, No. 5834, pp. 83-86, 2007.

[2] M. M. Thackeray, C. Wolvertonb and E. D. Isaacs, “Electrical energy storage for transportation—approaching the limits of, and going beyond, lithium-ion batteries,” Energy Environ. Sci., 2012, vol. 5 , 7854 -7863.

[3] M. Yilmaz and P. T. Krein, "Review of Battery Charger Topologies, Charging Power Levels, and Infrastructure for Plug-In Electric and Hybrid Vehicles," in IEEE Transactions on Power Electronics, vol. 28, no. 5, pp. 2151-2169, May 2013, doi: 10.1109/TPEL.20.

[4] D. Patil, M. K. McDonough, J. M. Miller, B. Fahimi and P. T. Balsara, "Wireless power transfer for vehicular applications: Overview and challenges", IEEE Transactions on Transportation Electrification, vol. 4, no. 1, pp. 3-37, 2018.

[5] P. D. Aghcheghloo, D. J. Wilson and T. Larkin, "Towards the Electrification of Road Infrastructure," Equity in Transportation, New Zealand, Mar. 2020.

[6] S. Li and C. C. Mi, "Wireless Power Transfer for Electric Vehicle Applications," in IEEE Journal of Emerging and Selected Topics in Power Electronics, vol. 3, no. 1, pp. 4-17, March 2015..

[7] A. A. S. Mohamed, C. R. Lashway and O. Mohammed, "Modeling and Feasibility Analysis of Quasi-Dynamic WPT System for EV Applications," in IEEE Transactions on Transportation Electrification, vol. 3, no. 2, pp. 343-353, June 2017.

[8] G. N. Jordbakke, A. H. Amundsen, I. Sundvor, E. Figenbaum, I. B. Hovi, "Technological maturity level and market introduction timeline of zero-emission heavy-duty vehicles," The Institute of Transport Economics (TOI), 2018.

[9] R. Tavakoli and Z. Pantic, "Analysis Design and Demonstration of a 25-kW Dynamic Wireless Charging System for Roadway Electric Vehicles", IEEE Journal of Emerging and Selected Topics in Power Electronics, Sep 2018.

[10] Y. J. Jang, S. Jeong and Y. D. Ko, "System optimization of the On-Line Electric Vehicle operating in a closed environment", ScienceDirect, Comput. Ind. Eng., vol. 80, pp. 222-235, Feb. 2015.

[11] H. Fujimoto, O. Shimizu, S. Nagai, T. Fujita, D. Gunji and Y. Ohmori, "Development of Wireless In-wheel Motors for Dynamic Charging:

From 2nd to 3rd generation," IEEE PELS Workshop on Emerging Technologies: Wireless Power (WoW), Korea, pp. 56-61, 2020.

[12] K. Sasaki, T. Imura, “Combination of Sensorless Energized Section Switching System and Double-LCC for DWPT,” 2020 IEEE PELS Workshop on Emerging Technologies; Wireless Power Transfer (WoW), nov.2020.

[13] O. C. Onar, J. M. Miller, S. L. Campbell, C. Coomer, C. P. White and L. E. Seiber, "A novel wireless power transfer for in-motion EV/PHEV charging," 2013 Twenty-Eighth Annual IEEE Applied Power Electronics Conference and Exposition (APEC), Long Beach, CA.

[14] B. J. Limb et al., "Economic Viability and Environmental Impact of In-Motion Wireless Power Transfer," in IEEE Transactions on Transportation Electrification, vol. 5, no. 1, pp. 135-146, March 2019.

[15] S. Jeong, Y. J. Jang, D. Kum and M. S. Lee, "Charging Automation for Electric Vehicles: Is a Smaller Battery Good for the Wireless Charging Electric Vehicles?," in IEEE Transactions on Automation Science and Engineering, vol. 16, no. 1, Jan. 2019.

[16] E. Sproul et al., "Electrification of Class 8 Trucking: Economic Analysis of In-Motion Wireless Power Transfer Compared to Long-Range Batteries," 2018 IEEE Transportation Electrification Conference and Expo (ITEC), 2018, pp. 744-748, doi: 10.1109/ITEC.2018.

[17] M. Ziyadi, H. Ozer, S. Kang, I. L. Al-Qadi, "Vehicle energy consumption and an environmental impact calculation model for the transportation infrastructure systems," Journal of Cleaner Production,Volume 174, 2018, Pages 424-436.

[18] https://www3.nissan.co.jp/vehicles/new/leaf.html

[19] https://www.isuzu.co.jp/product/elf/

[20] https://www.isuzu.co.jp/product/forward_post/index.html

[21] https://www.hino.co.jp/selega/

[22] https://www.isuzu.co.jp/product/giga/

[23] J. Asamer, A. Graser, B. Heilmann, M. Ruthmair, "Sensitivity analysis for energy demand estimation of electric vehicles," Transportation Research Part D: Transport and Environment,Volume 46,2016,Pages 182-199.

[24] K. Holmberg, P. Andersson, N. O. Nylund, K. Mäkelä, A. Erdemir, "Global energy consumption due to friction in trucks and buses,"Tribology International,Volume 78, 2014.

[25] SEMI:https://www.tesla.com/semi, TESLA.

[26] Y. Yamada, T. Imura, "A study on Optimization of Wireless Power Transmission Ferrite-less Coils in the 85 kHz Band by Numerical Analysis," EVTeC2021, Yokohama, 2021, May.

[27] Yuto Yamada Takehiro Imura, "Maximum Output Power Design Considering the Efficiency in Wireless Power Transfer Coils", 47th Annual Conference of the IEEE Industrial Electronics Society (IECON2021), Oct.2021.

[28] SAE International, “Wireless Power Transfer for Light-Duty Plug-in/Electric Vehicles and Alignment Methodology J2954, ” Issued2016-05, Revised2020-10

[29] C. Cuevas, S. Declaye, V. Lemort, "Experimental characterization of a reversible heat pump for hybrid and electric vehicles," Advances in Mechanical Engineering, Apr 2019.

[30] Y. Yamada, T. Imura, "A Simplified Model of The Power Requirement and Battery Level for Dynamic Wireless Power Transfer by Various Vehicles," The Institute of Electrical Engineers of Japan (IEEJ), Automotive/Transportation and Electric Railways, 2021 Sep.

[31] K. Hanawa, T. Imura and N. Abe, "Basic Evaluation of Electrical Characteristics of Ferrite-less and Capacitor-less Coils by Road Embedment Experiment for Dynamic Wireless Power Transfer," IEEE PELS, WoW, pp.1-5, 2021